Calibration of the ALFRESCO Simulation Model with a Grassland Module for the Kanuti National Wildlife Refuge

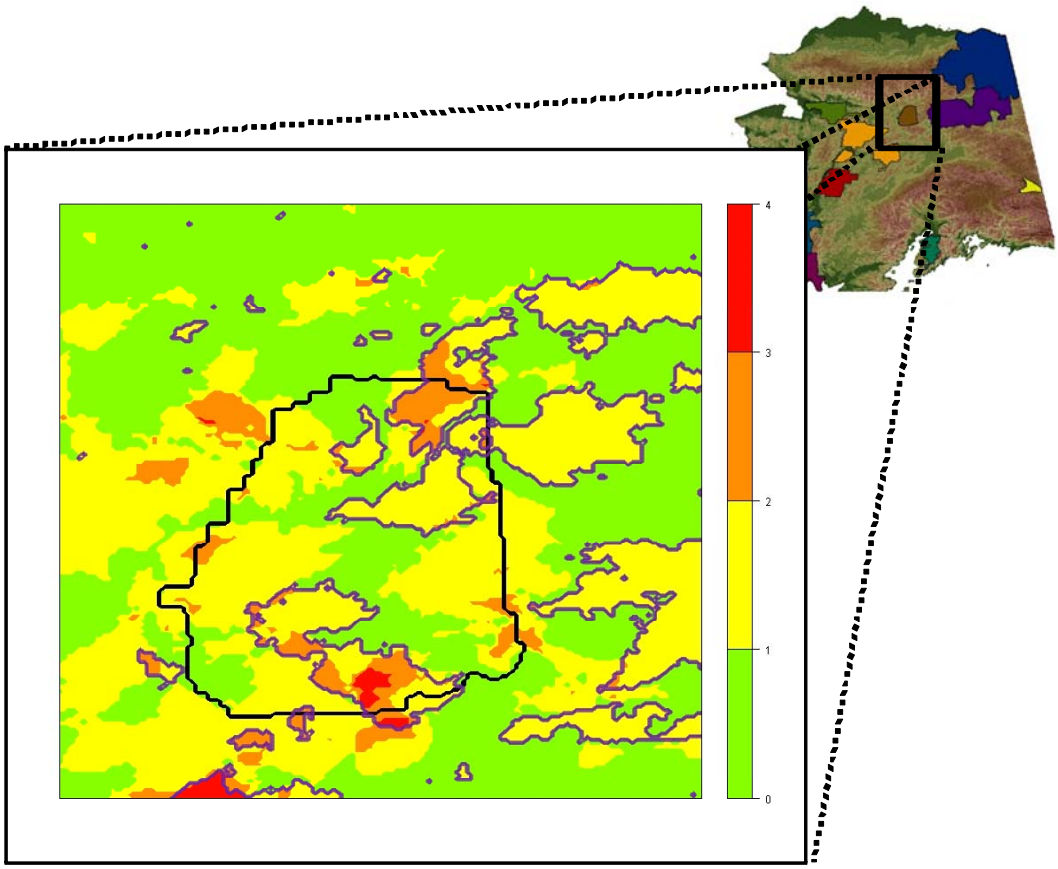

T. Scott Rupp, and Mark Olson, University of Alaska Fairbanks

Paul Duffy, Neptune and Company, Inc.

Prepared for U.S. Fish and Wildlife Service

National Wildlife Refuge System

January 1, 2011

Abstract

Interest in the emergence of graminoid vegetation as a dominant ecosystem type across Alaska has recently increased. This is due to both analysis of remotely sensed vegetation products and anecdotal observations from field work. This work serves as a component of a larger effort to provide a framework for the iterative interaction of data collection and simulation modeling. This framework is a means to the end of quantitatively characterizing and testing hypotheses about the linkages among climate, fire and grassland vegetation in Alaskan ecosystems. We use the Kanuti National Wildlife Refuge as a test domain to analyze and implement information from historical data on fire, climate and vegetation. This information is then implemented into the ALFRESCO modeling framework to develop a novel grassland frame. This new model version is then calibrated using the historical data. The most novel result from this work is that anomalously high post-fire dominance by graminoid vegetation appears to be correlated with anomalously high precipitation in the years following fire events. This result is based on very limited data; however it does provide an interesting juxtaposition to the previously developed conceptual model. Future work will focus on the analysis of similar datasets for other regions within Alaska in order to determine if this post-fire climatic signature is robust. The modeling framework developed here allows for a relatively simple assimilation of new data to inform the interactions among fire, climate and graminoid vegetation in Alaska.

Introduction

The goal of this task is to calibrate a version of the Alaska Frame-Based Ecosystem Code (ALFRESCO) simulation model that includes a novel vegetation frame accounting for graminoid-dominated areas, referred to hereafter as “grassland”. This new model version characterizes the emergence of grasslands in the context of a conceptual model developed in a previous task (Figure 1). The conceptual model is updated based on data analysis performed as part of this task and the result is implemented into the definition of the novel grassland frame. The new model version is tested on a domain centered on the Kanuti National Wildlife Refuge (NWR) landscape, a boreal ecosystem dominated by both black and white spruce (*Picea mariana* and *P. glauca*, respectively) as well as aspen (*Populus tremuloides*) and birch (*Betula neoalaskana*) stands (Figure 2). The primary deliverable from this task is a functional ALFRESCO version suitable for application on the spatial domain of the Kanuti NWR.

Methods

This calibration work utilizes information from the conceptual model in conjunction with analyses of historical data regarding the spatial distributions of fire, vegetation, and topography. Based on the previously developed initial conceptual model, the combination of fire and anomalous post-fire temperature/precipitation was hypothesized to be a main driver allowing for grassland vegetation to emerge on the landscape. Specifically, the combination of low precipitation and high temperature was considered to favor the grassland vegetation type. Impacts of climate on post-fire recruitment of the grassland vegetation type were analyzed using data from the Western Regional Climate Center station data for Bettles, AK (http://www.wrcc.dri.edu/summary/Climsmak.html). For information regarding the spatial distribution of vegetation types, the National Land Cover Database data product (NLCD 2001:

http://www.mrlc.gov/nlcd_definitions.php) was utilized. For the purpose of classifying grassland vegetation in this ALFRESCO version, we aggregated the vegetation classes denoted as 51 (Alaska dwarf scrub), 71 (grassland/herbaceous), and 72 (Alaska sedge herbaceous) from the NLCD 2001. This resulted in 8.1% of the simulation landscape being classified as grassland vegetation. Within this 8%, 78% corresponded to Alaska dwarf scrub, 5% corresponded to grassland/herbaceous, and 17% are sedge herbaceous. These three classes in the NLCD correspond to the single grassland frame in ALFRESCO. Information regarding historical fire activity was obtained from the Alaska large fire database (http://fire.ak.blm.gov/incinfo/aklgfire.php).

Slope and aspect information from a digital elevation model (DEM) were used to quantify the topographical influence on interactions among fire, post-fire climate, and grassland vegetation (Figures 3 and 4). Figure 3 shows the spatial distribution of the grassland vegetation overlaid on a spatially explicit representation of slope information from the DEM. Slope is considered as a binary variable (i.e., hilly or flat) for each pixel based on a cutoff of 1.5 degrees. The majority of grassland vegetation exists on non-flat regions. Aspect has an interactive effect with slope. In order to assess the distribution of grassland vegetation as a function of the interactive effects of slope and aspect we created an indicator variable that increases by a unit value for either: 1) non-South-facing or 2) significant (i.e. hilly) slopes. Any pixel on the landscape with an aspect between 135 degrees (SE) and 225 degrees (SW) is represented in red and is considered to be South-facing (Figure 4). Other aspects are represented in green. The majority of the grassland pixels are in the green region and specifically, 79% of grassland cells are on aspects greater than 225 degrees (SW) and less than 135 degrees (SE) (e.g. not South-facing). Figure 5 and Table 1 show the interactive impacts of slope and aspect; only 4% of the grassland vegetation exists in areas that are South-facing with slope<1.5%.

In the ALFRESCO model, black spruce is primarily restricted to non-South facing aspects or area with little to no slope. Hence, the grassland frame is developed as a subset of the black spruce frame based on these analyses relating the spatial distribution of grassland vegetation on the landscape to topographic characteristics. This was largely consistent with the observed spatial distribution of the grassland vegetation in the Kanuti NWR. Additional characteristics of the grassland frame (e.g. relative flammability, probability of post-fire emergence as a function of burn severity) were quantitatively characterized using similar data analyses, literature review, and subject matter expert opinion. Data needed to fill gaps in the conceptual model are relatively sparse, so informing the grassland frame will be an ongoing and iterative activity as new field data become available.

The goal of this work is not to provide a perfect representation of the grassland frame in the Kanuti NWR. However, it is possible to provide a representation that produces results that are consistent with the system, and also provides a framework for the assimilation of subsequent data collection activities or relevant information from the literature. The latter is critically important, in that it allows for the iterative interaction among data and models that ultimately provides the most effective use of past data to resolve the most pressing data gaps.

Analyses to Inform Calibration Efforts

The data analysis used to inform the calibration of the grassland can be broken out into analyses of two datasets: pre-2001 fire activity and post-2001 fire activity. The use of this timeframe is driven by the 2001 vegetation map from the NLCD. In this context, the intersection of the cumulative fire activity map with the distribution of grassland across the landscape at 2001 provides a dataset that can be used to quantify the relative importance of fire in the subsequent emergence of grassland vegetation. Additionally, the intersection of the fires from 2001-2010 with the 2001 NLCD grassland classifications provides some information regarding the relative likelihood of grassland vegetation burning (Figure 6). Specifically, the probability of grassland burning seems to be roughly equal to the relative proportion of grassland on the landscape. Hence there is no reason to initialize the flammability of the grassland frame with values that are too different from those of the corresponding forest vegetation. Although there is a substantial amount of grassland vegetation that exists on the landscape outside of the fire perimeters from 1940-2010, these areas will require additional data collection through field studies to assess the interactions among fire/disturbance, climate, and vegetation beyond assumptions made as part of this conceptual model and data analysis.

Spatially explicit fire records for the period 1940-2010 were represented on a $1km^2$ spatial resolution grid that is spatially consistent with the 2001 NLCD vegetation map, also at $1km^2$ resolution. Since the vegetation data are currently only available as a snapshot for year 2001, fire data for this portion of the analysis were only analyzed from 1940-2000. Specifically, the combination of the 2001 NLCD vegetation map and the historical fire information was used to identify and characterize areas where both of the following conditions were met: 1) fires burned prior to 2001, and 2) the 2001 vegetation map identifies the vegetation type as either Alaska dwarf scrub, grassland/herbaceous or sedge/herbaceous.

Figure 6 shows the cumulative fire activity with the spatial distribution of grassland vegetation superimposed. Figure 4 and Table 2 show that approximately 8% of the simulation region is considered grassland at 2001. At first inspection, there is not any striking pattern that suggests strong spatial correlation of the existence of grassland vegetation with historical fire activity; however, there are several of the larger fires on the map that coincide with large contiguous patches of grassland vegetation. The historical fire perimeters that contain these contiguous patches of grassland vegetation correspond to the years 1990 (Figure 7) and 1997 (Figure 8). In particular, roughly 50% of the 1997 fire activity is classified as grassland vegetation on the 2001 NLCD vegetation map. We therefore focus on the 1997 data to characterize the climatic signal associated with this anomalously large post-fire grass recruitment.

Using the subset of grassland sites that burned prior to the creation of the 2001 vegetation map, the impact of post-fire climate on the likelihood of subsequent grassland dominance was quantified (Table 2). Several important pieces of information emerge from Table 2. First, the percentage of cells that exist in a grassland state after fire tends to be a number in the low single digits. Second, the exception to this is the 1997 fire, which was followed by several exceptionally wet years (Figure 9). This result is in opposition to the preliminary conceptual model, which suggested those hot and dry years after fire would favor grassland development.

The quantification of impacts of burn severity and impacts of post-fire climate on grassland emergence were done as simply as possible. Given the relatively sparse information regarding these dynamic interactions among climate fire and grassland vegetation, simpler models are more useful in terms of understanding the relative impacts of assumptions. That said, we have constructed the grassland frame to easily allow for more complex linkages between fire and post-fire climate. For example, ALFRESCO currently simulates fires with varying fire severity. The probability of grassland emergence after fire is allowed to vary as a function of both fire severity and the existence of grassland prior to the fire event. This functionality is established in accordance with the conceptual model; however, there is little quantitative information to suggest the relative impacts of fire severity and the existence of pre-fire grassland on the post-fire emergence of a dominant grassland vegetation type. Consequently, we have left these transition probabilities relatively equal across burn severity and pre-fire vegetation types. Subsequent new data sources or regions outside the Kanuti NWR may provide meaningful quantitative information to better inform this grassland frame.

The grassland frame was also designed to account for anomalous post-fire climatic signals in the calculation of the probability of post-fire grassland emergence. The requirements for years that provide bounding cases are: a non-trivial amount of area burned, the fire occurred relatively recently (in order to minimize impacts from a long time period between the time of the fire and the time of the classified NLCD imagery), and that post-fire grassland vegetation was either very high or very low. The first bounding case we consider is the 1997 fire NE of Bettles. This fire burned 9,750 ha and the post-fire vegetation was roughly 50% grassland vegetation (Table 2, Figure 8). As a middle-of-the-road case where an average percentage of post-fire vegetation is grassland, we consider year 1990 when roughly 7% of the post-fire vegetation was grassland (Table 2, Figure 7). As a next step, we examined the growing season temperature and precipitation for the years following these fire years to provide an initial quantification of the climate impact on post-fire grassland emergence.

According to the conceptual model, the existence of hot and dry conditions would favor the post-fire emergence of grassland vegetation; however, our data analysis suggests the opposite effect. Specifically, the 1997 fire year had the largest post-fire recruitment of grass and also experienced several of the wettest summers on record in 1998 and 1999. This effect was accommodated by allowing for the precipitation in subsequent years to increase the probability of a transition to grassland after a fire. There is uncertainty as to the duration of time after a fire that the summer temperature and precipitation can meaningfully impact the probability of post-fire grassland emergence. Because of this, the number of years that the climate after a fire is considered can be specified by the model user.

Fire and Grassland Calibration Results

In addition to a suite of calibration metrics used to ensure realistic depiction of the regional fire regime (Appendix A), the main additional calibration metric used for this activity is percentage of grassland vegetation on the 2001 landscape in the context of historical fire activity (Figure 10). The results in Appendix A show that this version of ALFRESCO does a good job of depicting simulated fires on the landscape in a manner that is consistent with the historical fire activity.

The main determinants of differences (among the simulated landscape and the observed historical activity) are stochasticity in the spatial location of ignitions, the distribution of differentially flammable vegetation types, and the quantification of the factors that are relevant to grassland emergence. These are accounted for through the simulation of numerous different replicates of the landscape. Results from the collective set of replicates are used to account for these multiple sources of unresolved uncertainty in the simulation model.

Discussion and Future Work

Although the data used in this analysis provide the best information currently available, there are some aspects of the characterization of linkages among topography, fire, and post-fire vegetation that are uncertain. Specifically, we only have a snapshot of vegetation state for one year over the analysis period. Hence we cannot account for changes in the importance of topography and post-fire climate on vegetation state through time. Consequently, as a first step, we make assumptions about the stability of these relationships for the implementation of the conceptual model regarding the emergence of grassland on the landscape. The use of additional remotely sensed products in conjunction with field verification of the NLCD classifications would provide important information to revise the dynamics of this grassland frame.

One of the advantages of working with this type of simulation framework is that assumptions of the model can be tested and revised as simulation results and new data provide evidence either for or against assumptions of the model. With the assumption that the linkages among topography, fire, and post-fire climate remain roughly stable through time, we considered several fire years that appear to characterize the envelope of favorable climate for the establishment of grassland on the landscape after fire. Our characterization of the impact of post-fire climate conditions was necessarily simplistic due to the relative paucity of data. Additional data products that may help refine these initial models include those provided by the Moderate Resolution Imaging Spectroradiometer (MODIS) Terra and Aqua platforms. These platforms provide land cover classification data using the International Geosphere Biosphere Program (IGBP) classification scheme for the period 2001-2007 (http://webmap.ornl.gov/wcsdown/dataset.jsp?ds_id=10004). These data may be useful for future work with respect to understanding year to year changes in post-fire vegetation dynamics within the Kanuti NWR.

Another large source of uncertainty in the current implementation of the grassland frame is the impact of burn severity. Burn severity is currently adequately modeled in this ALFRESCO version; however its impact on post-fire grassland emergence is likely oversimplified due to a lack of data. We have accommodated the availability of additional data to inform this part of the model through the implementation of a generalized calculation of transition probabilities that can be modified as a function of burn severity. The most useful next step toward addressing this issue would be to obtain either remotely sensed or possibly field-based estimates of the burn severity from the 1997 fire. This would allow for some additional quantification of the impact of burn severity on the probability of post-fire grassland emergence. An additional consideration is that these burn-severity patterns may have an interaction with post-fire climate. In order to

address this question, a dataset spanning a range of both burn severities and post-fire climate conditions would need to be assembled and analyzed.

Figure 1: State and transition diagram for ALFRESCO

The fire subroutine in ALFRESCO remains essentially unchanged with the exception of the estimation of flammability for the grassland frame. In all cases, the existence of the grassland frame is initiated by fire. After fire, the necessary and sufficient climatic conditions for the grassland frame are estimated based on data from the Kanuti NWR.

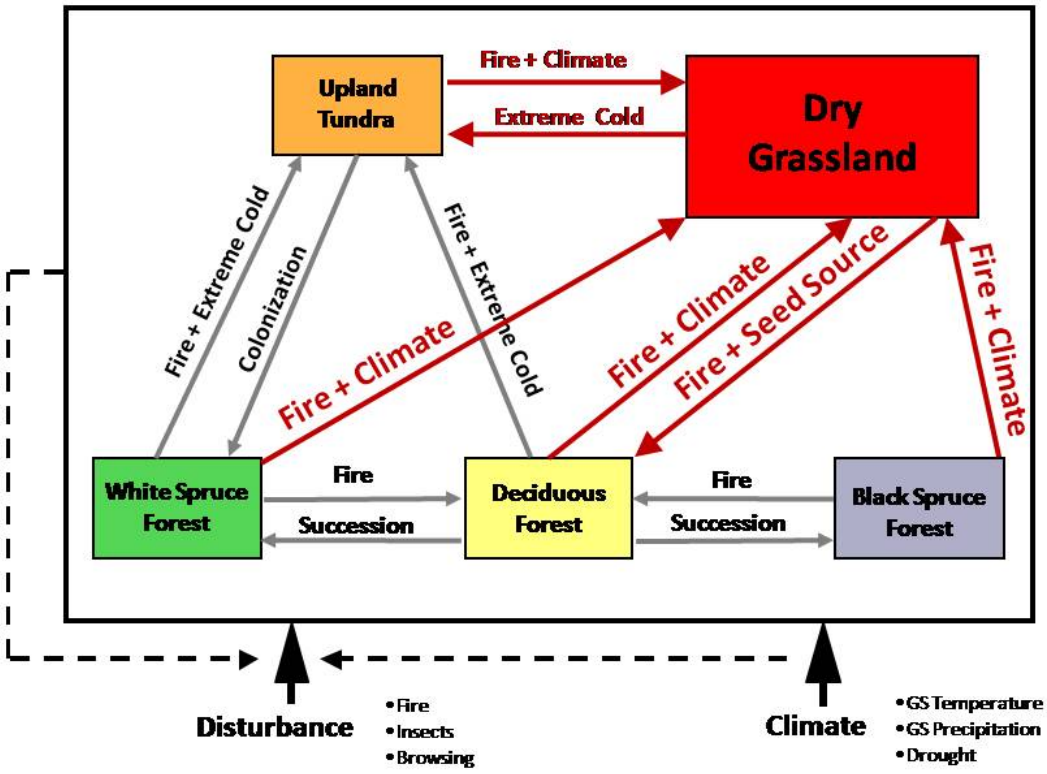

Figure 2: Spatially explicit map of fire activity from 1940-2010 for the Kanuti NWR. The legend shows the number of burns that have occurred in the period of interest. The square represents the buffered region of interest for the ALFRESCO modeling simulations. The buffer is used to minimize the "edge effects" that can occur from not allowing fires that ignite outside the region of interest to influence the edges. The simulation region is 179 km^2 wide and 159 km^2 high.

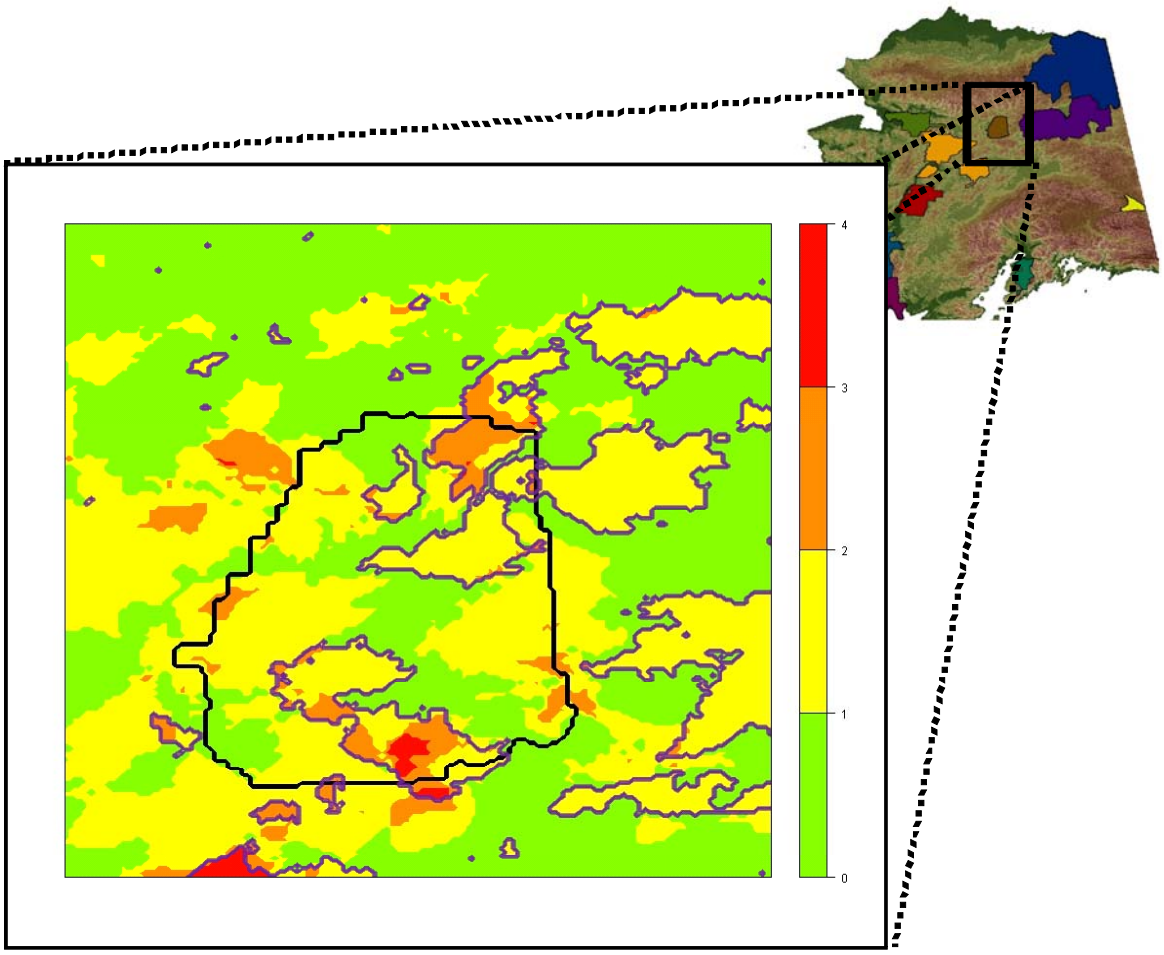

Figure 3: The spatial distribution of the grassland vegetation overlaid on a spatially explicit representation of slope information from the DEM. Slope is considered as a binary variable (hilly = red, flat = green) for each pixel based on a cutoff of 1.5 degrees.

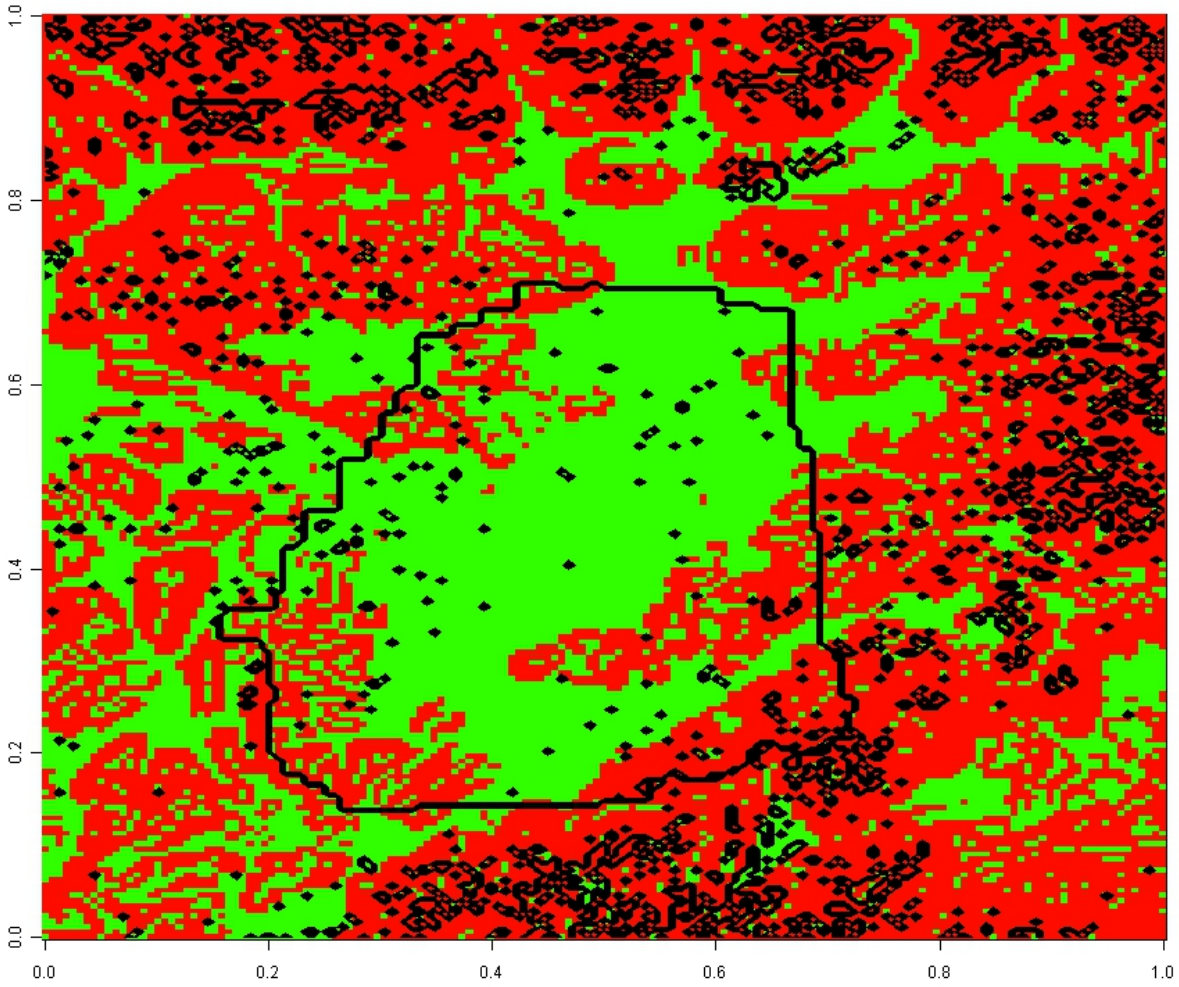

Figure 4: Spatial distribution of the grassland vegetation type overlaid on a map depicting aspect information for the Kanuti NWR. South facing areas are represented in red and correspond to regions where the aspect is both less than 225 degrees (SW) and greater than 135 degrees (SE). Roughly 80% of the grassland vegetation occurs in the green areas.

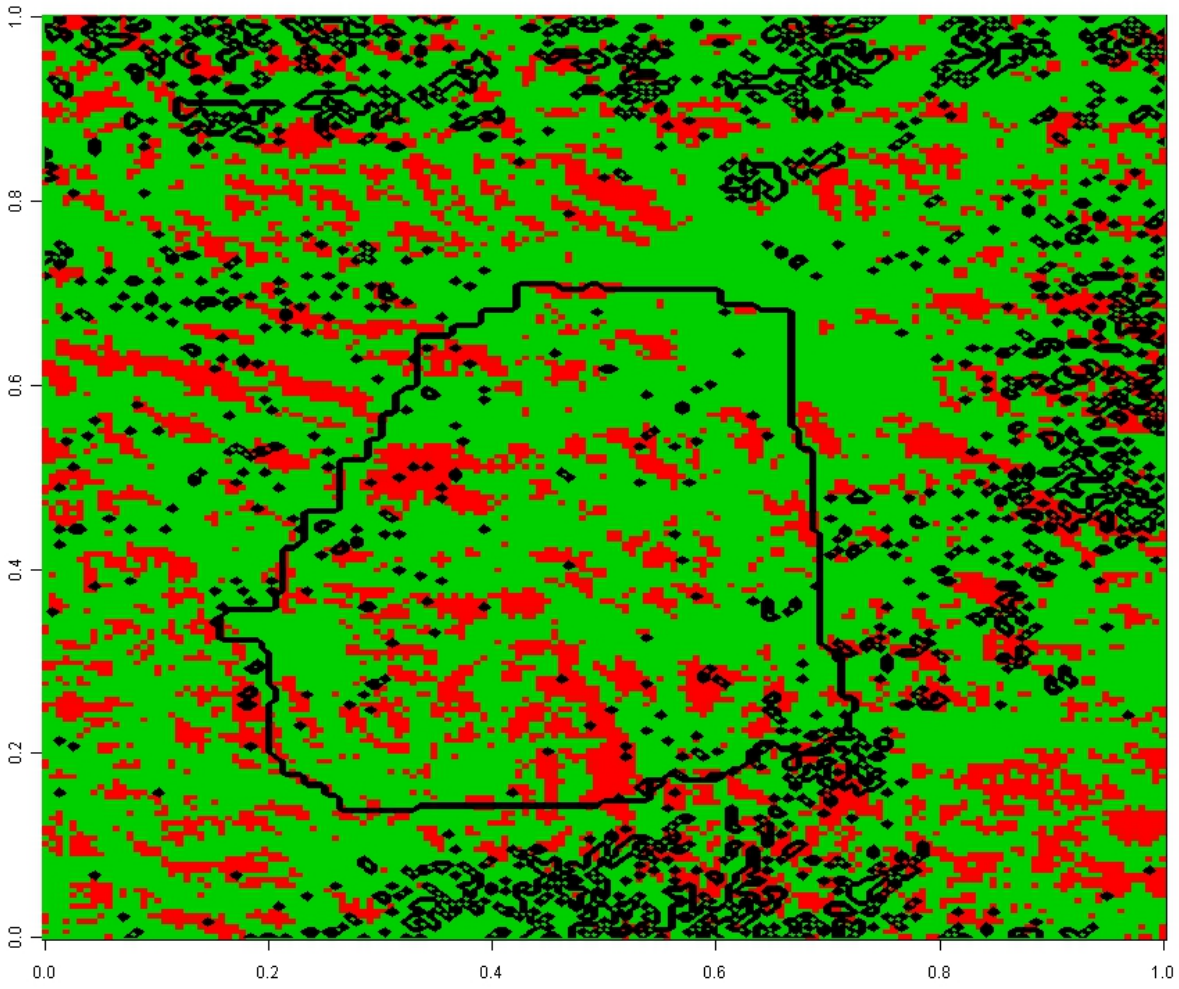

Figure 5: Spatial distribution of the grassland vegetation type overlaid on a map depicting combined slope and aspect information for the Kanuti NWR. Areas in red correspond to regions with minimal slope and the aspect is South (i.e., both less than 225 degrees (SW) and greater than 135 degrees (SE)). Yellow regions correspond to exclusively one of either 1) slope greater than 1.5 degrees or 2) the aspect is North (i.e., greater than 225 degrees (SW) or less than 135 degrees (SE)). Grassland vegetation is most common in the green areas, which are neither flat nor North.

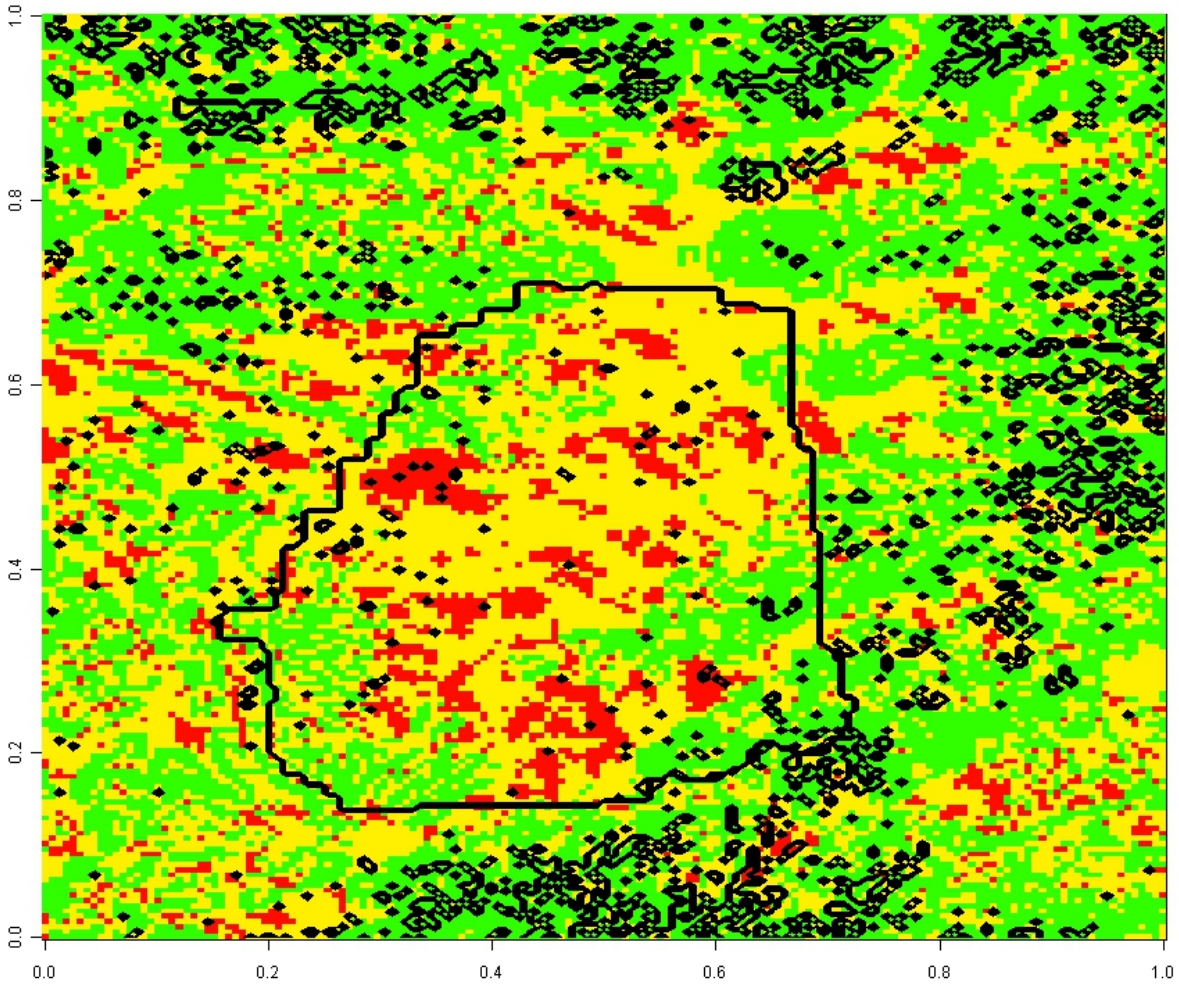

Figure 6: Spatial distribution of the grassland vegetation type overlaid on the cumulative fire map for years 1940-2010 for the Kanuti NWR. Grassland vegetation from the 2001 NLCD classification is depicted with the black circles. Scale represents the number of burning events. Fires prior to 2001 provide information about post-fire recruitment of grassland vegetation. Fires that burned after 2001 have a purple perimeter and provide information about the relative likelihood of grassland vegetation burning.

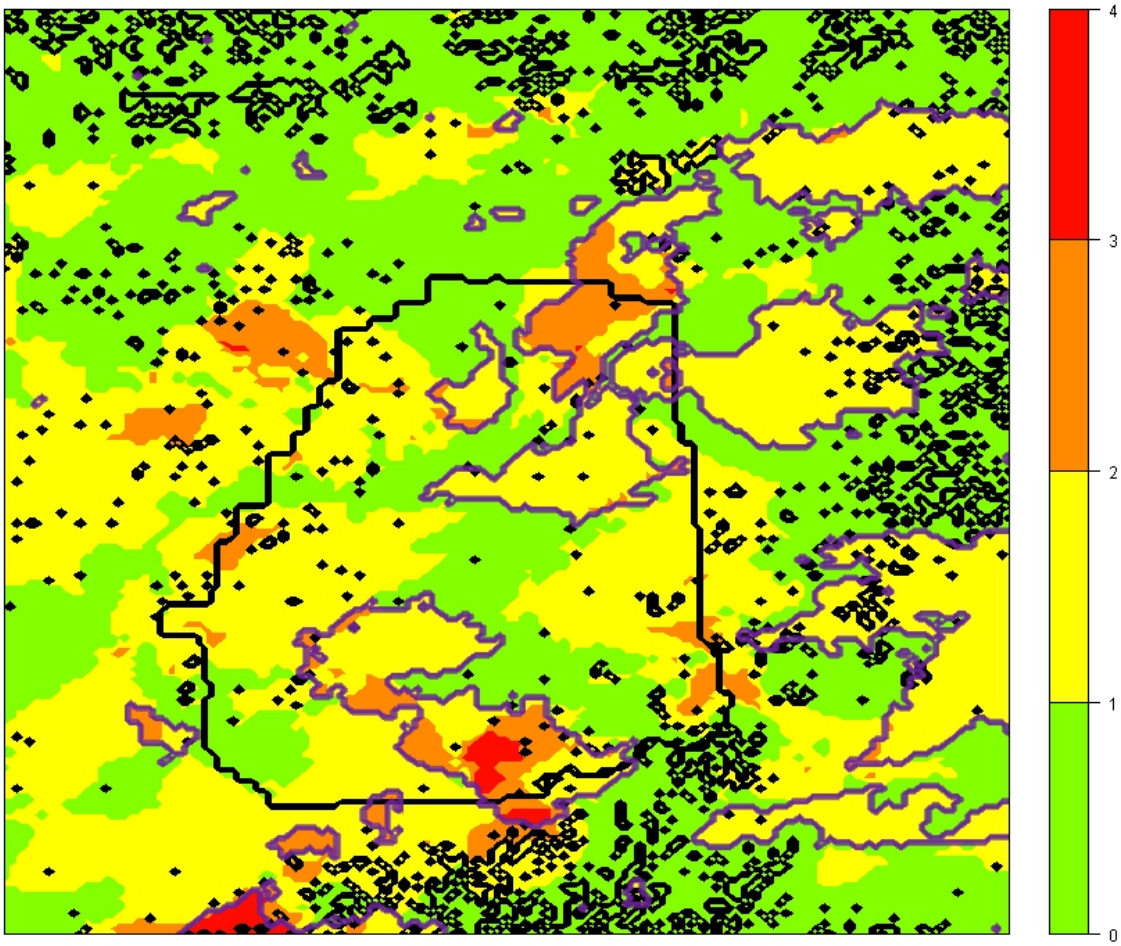

Figure 7: Spatial distribution of the grassland vegetation type overlaid on the 1990 fire map for the Kanuti NWR. Grassland vegetation is depicted with the black circles. Approximately 7% of the area burned in 1990 is classified as grassland by the 2001 NLCD vegetation classification map. This percentage is about average (Table 1).

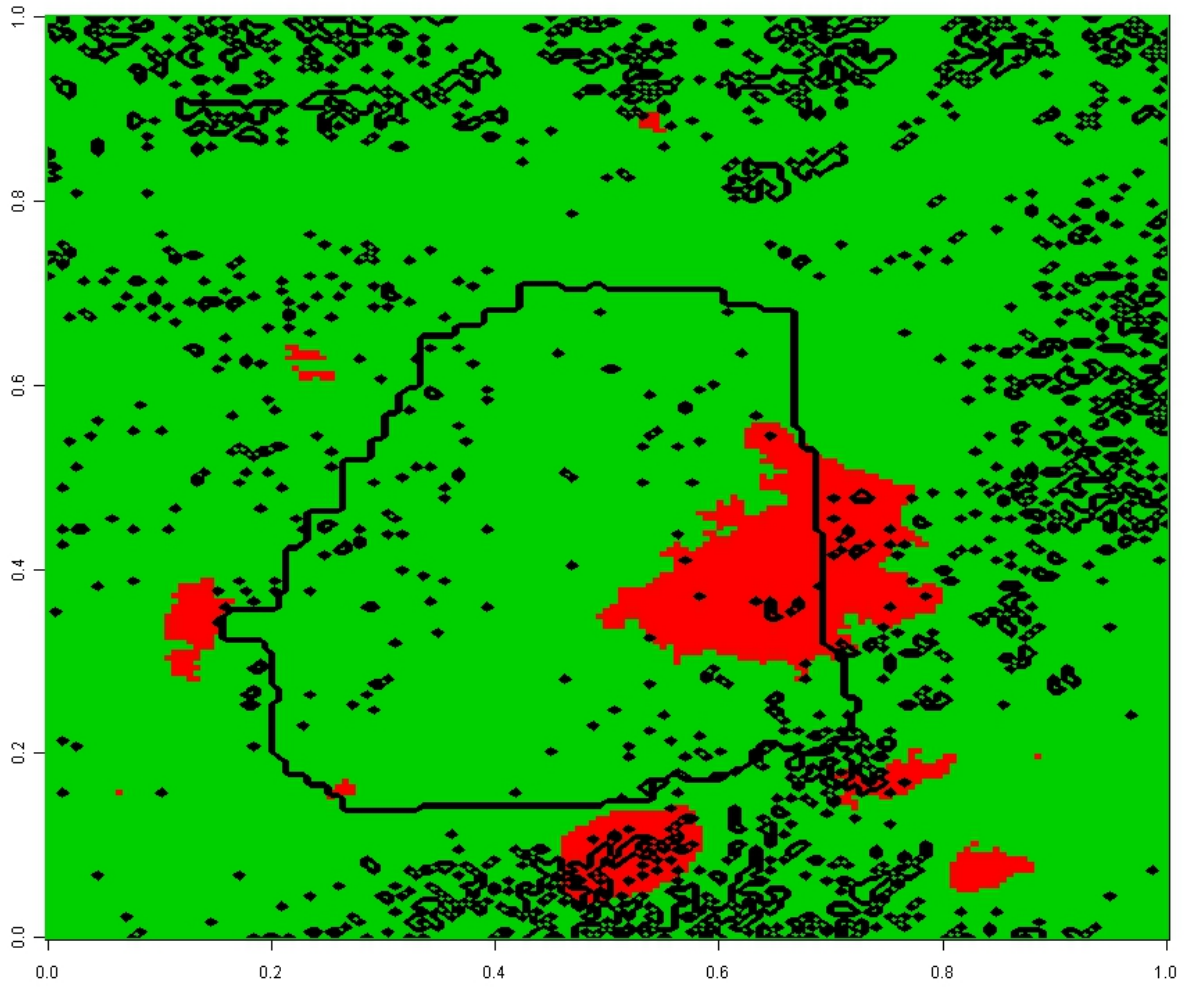

Figure 8: Spatial distribution of the grassland vegetation type overlaid on the 1997 fire map for the Kanuti NWR. Grassland vegetation is depicted with the black circles. Approximately 50% of the area burned in 1997 is classified as grassland by the 2001 NLCD vegetation map. This is the largest percentage for any of the years considered in this analysis (Table 1).

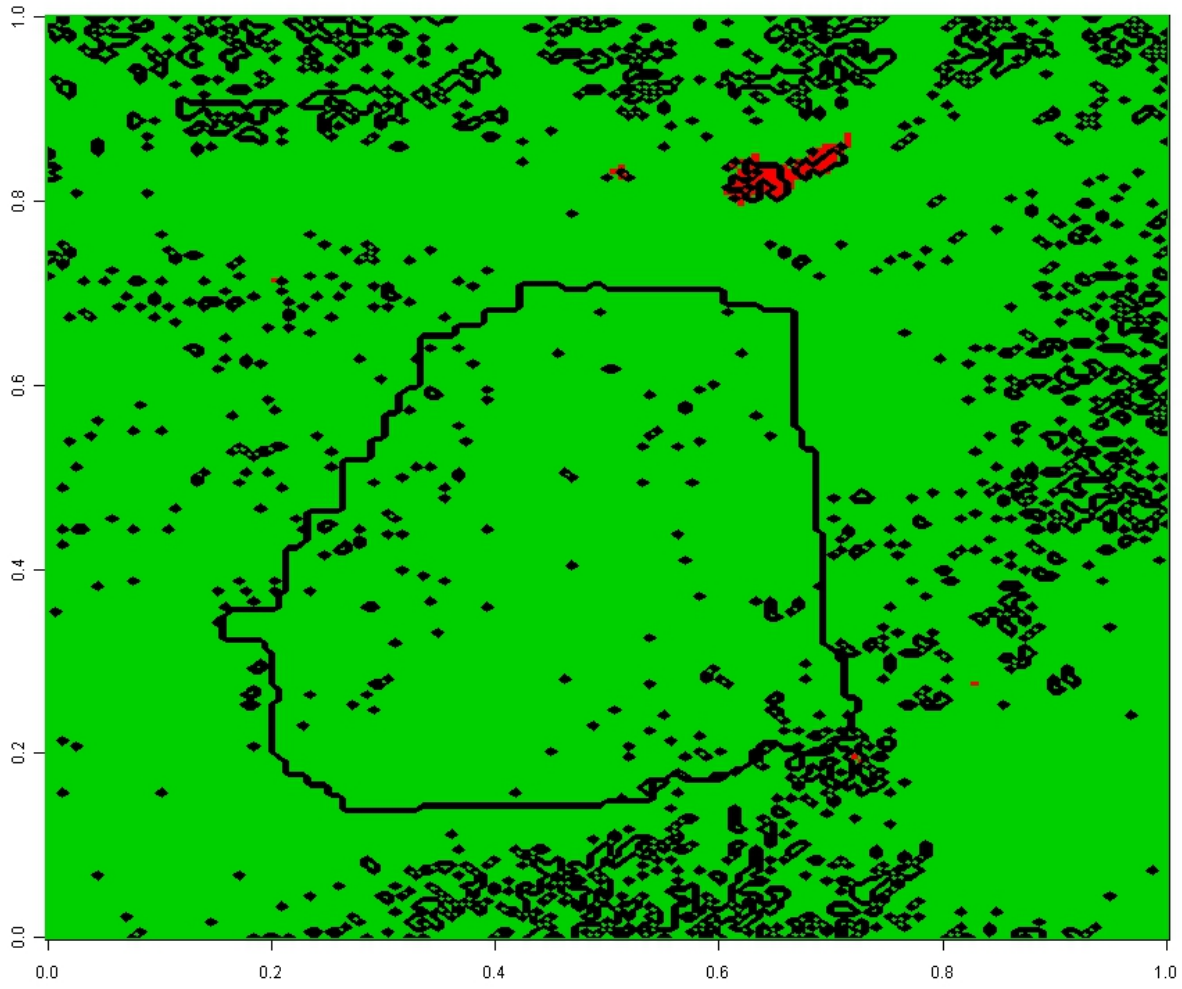

Figure 9: June and July precipitation for Bettles from 1950-2010. The years 1998 and 1999 are circled in red to show years after a recent fire where a majority of post-fire vegetation was grassland.

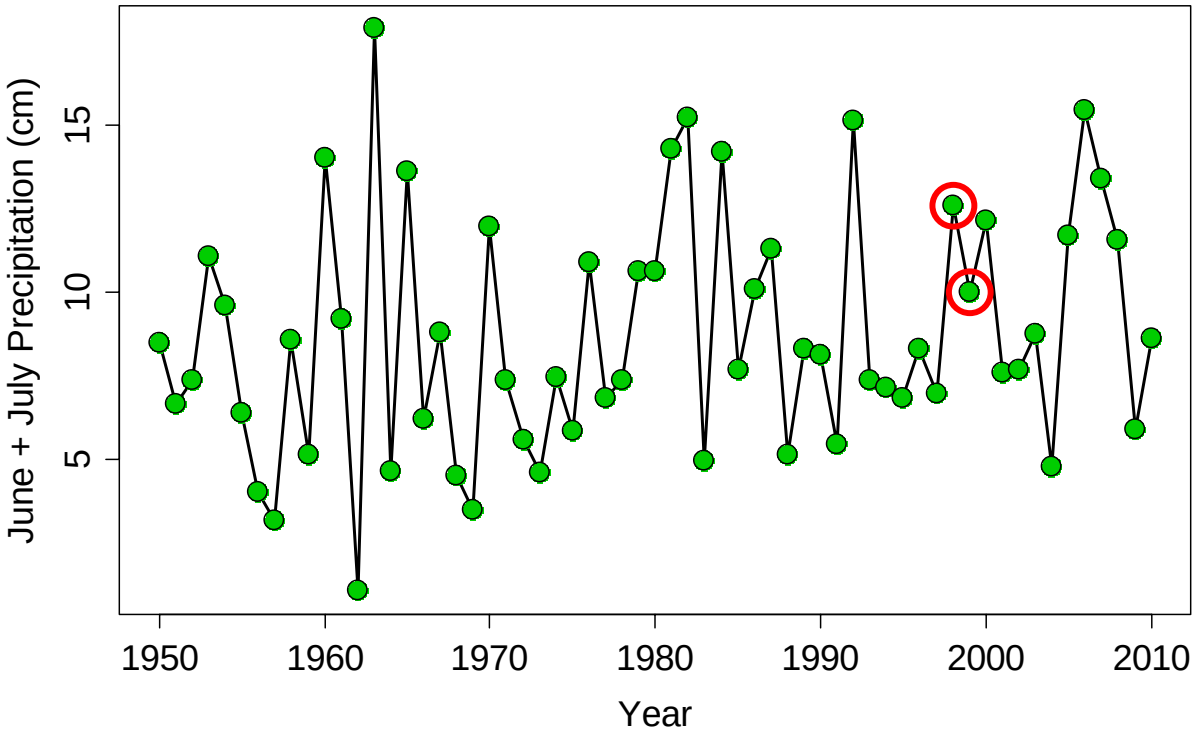

Figure 10: Historical versus simulated percentage of grassland on the Kanuti NWR simulation landscape for year 2001.

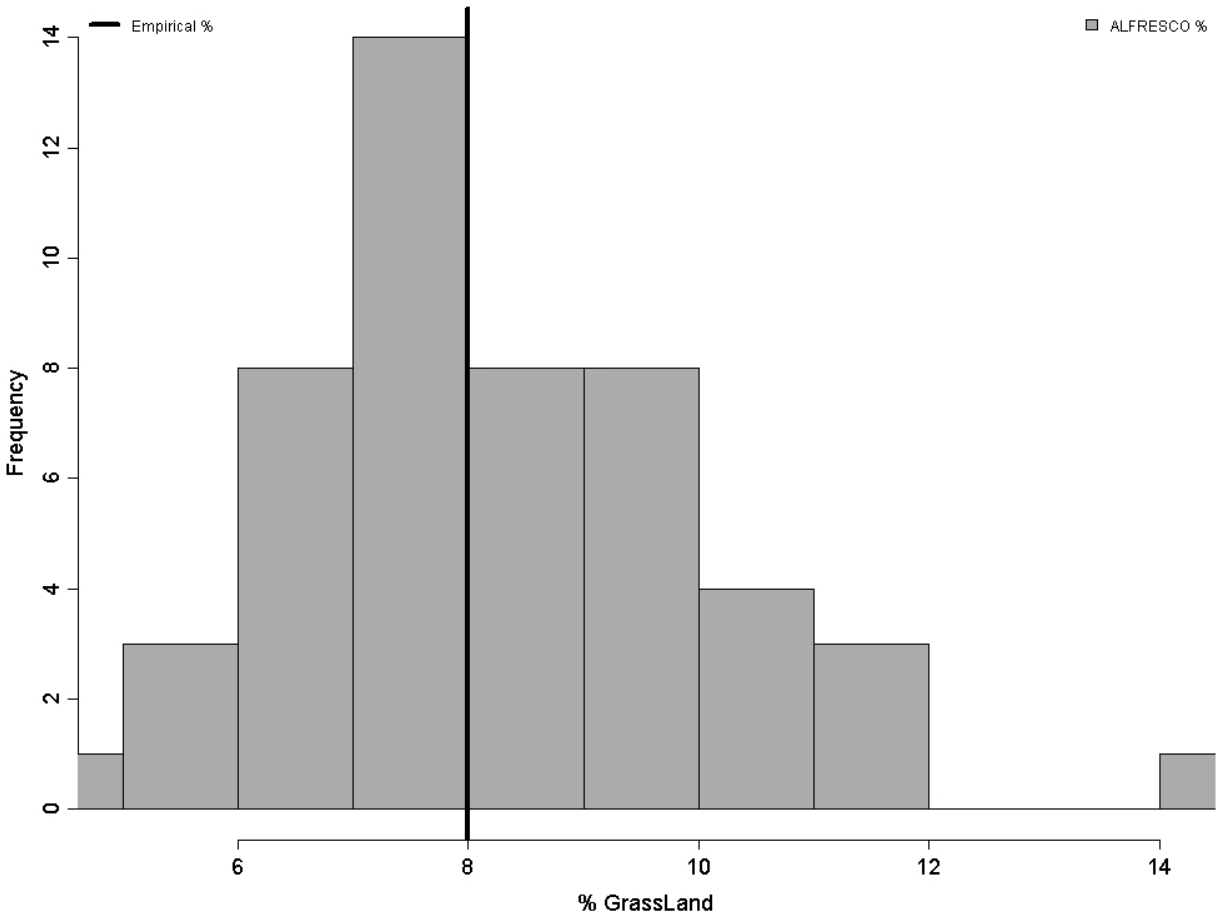

Table 1: Contingency table of the subset of pixels that contain grassland vegetation. Grassland percentages are broken out as a function of two factors: slope and aspect. Each factor has two levels. Slope is partitioned into two classes based on South (i.e., both less than 225 degrees (SW) and greater than 135 degrees (SE)) and not-South. Slope is partitioned simply into hilly (greater than 1.5 degrees based on a s DEM) and flat.

	Hilly	Flat	Total
South	15%	4%	19%
Not South	66%	14%	81%
Total	82%	18%	100

Table 2: Area burned annually with computed percentage of annual area burned that is classified as the grassland vegetation type according to the 2001 NLCD vegetation classification product. 'NA' indicates that 0 km^2 burned in a given year.

Year	km^2 Burned	% Burned Area that is Grassland in 2001
1940	0	NA
1941	0	NA
1942	0	NA
1943	0	NA
1944	0	NA
1945	0	NA
1946	**364**	**0%**
1947	0	NA
1948	0	NA
1949	0	NA
1950	**129**	**9%**
1951	0	NA
1952	0	NA
1953	**62**	**2%**
1954	**245**	**7%**
1955	0	NA
1956	**5**	**0%**
1957	**357**	**7%**
1958	0	NA
1959	**139**	**0%**
1960	0	NA
1961	0	NA
1962	0	NA
1963	0	NA
1964	0	NA
1965	0	NA
1966	0	NA
1967	0	NA
1968	**375**	**2%**
1969	**4591**	**3%**
1970	0	NA
1971	**1**	**0%**
1972	**1259**	**3%**
1973	0	NA
1974	0	NA
1975	0	NA

Year	km^2 Burned	% Burned Area that is Grassland in 2001
1976	0	NA
1977	**377**	**5%**
1978	0	NA
1979	0	NA
1980	0	NA
1981	**221**	**7%**
1982	0	NA
1983	0	NA
1984	**16**	**0%**
1985	**6**	**0%**
1986	0	NA
1987	0	NA
1988	**67**	**0%**
1989	0	NA
1990	**1774**	**8%**
1991	**1441**	**4%**
1992	**121**	**10%**
1993	**6**	**0%**
1994	**74**	**4%**
1995	**1**	**0%**
1996	0	NA
1997	**105**	**57%**
1998	0	NA
1999	3	0%
2000	19	0%
Pre-2001 Average	193	5%
2001	0	NA
2002	**105**	**0%**
2003	0	NA
2004	**2154**	**4%**
2005	**2778**	**4%**
2006	0	NA
2007	**22**	**5%**
2008	**21**	**5%**
2009	**73**	**15%**
2010	**200**	**0%**
Post-2001 Average	535	5%

Appendix A: Calibrations results related to the Fire Regime

Figure A-1: Historical and simulated cumulative area burned through time. Across the 50 different model runs, the average cumulative area burned is consistent with that observed from the historical record.

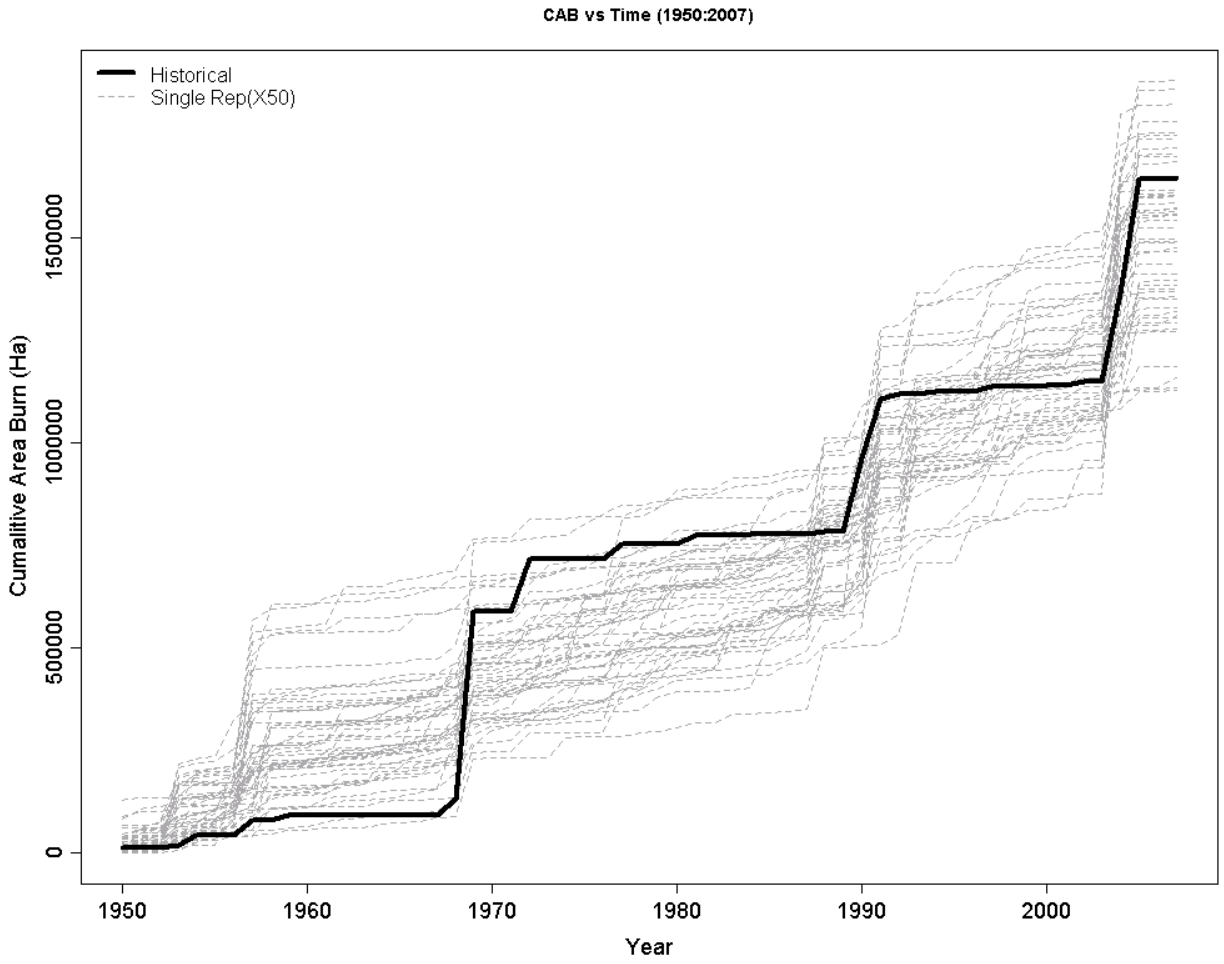

Figure A-2: Historical and empirical cumulative area burned as a function of fire size event. Across the 50 different model runs, the frequency versus area distribution of the fires sizes and the maximum fire size (vertical axis) are consistent with the observed historical data.

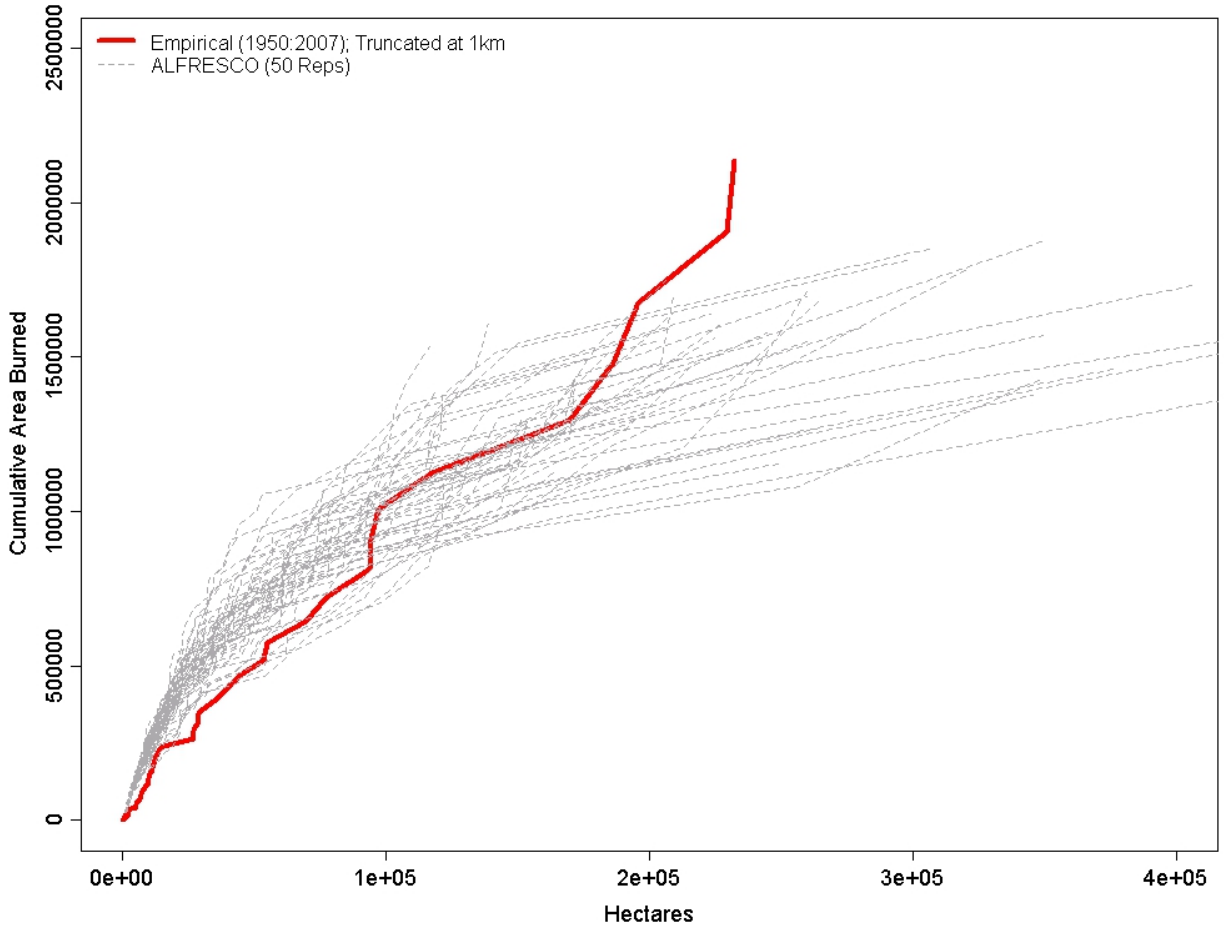

Figure A-3: Observed area burned for 2004 and 2005 (vertical black lines) and histograms for the 50 different model results for each year. These two years had significant area burned and an important calibration metric for the simulation results is the ability of ALFRESCO to pick up the fire activity that is a function of the climate signals in each of these years. In general, the model does a good job of representing these significant fire events.

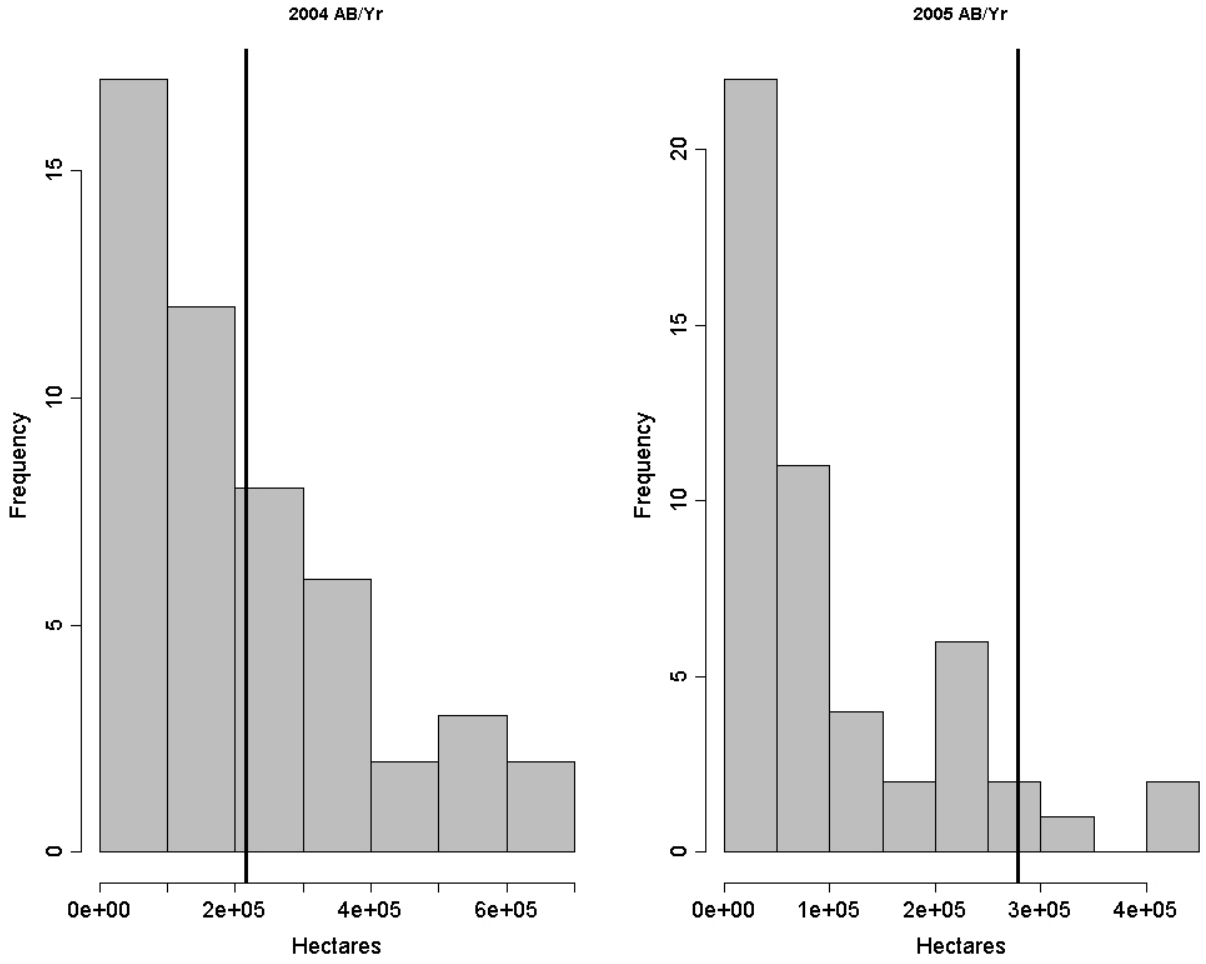

Figure A-4: Several different methods of computing the correlation between the area burned for the historical record and the 50 different simulation results. The fire activity in any given simulation is conditional on the spatial configuration of the differentially flammable vegetation types. In addition, there is stochasticity associated with the random ignitions in the simulation model. In the context of these sources of uncertainty, the simulation results are, on average, well aligned with the historical annual area burned.

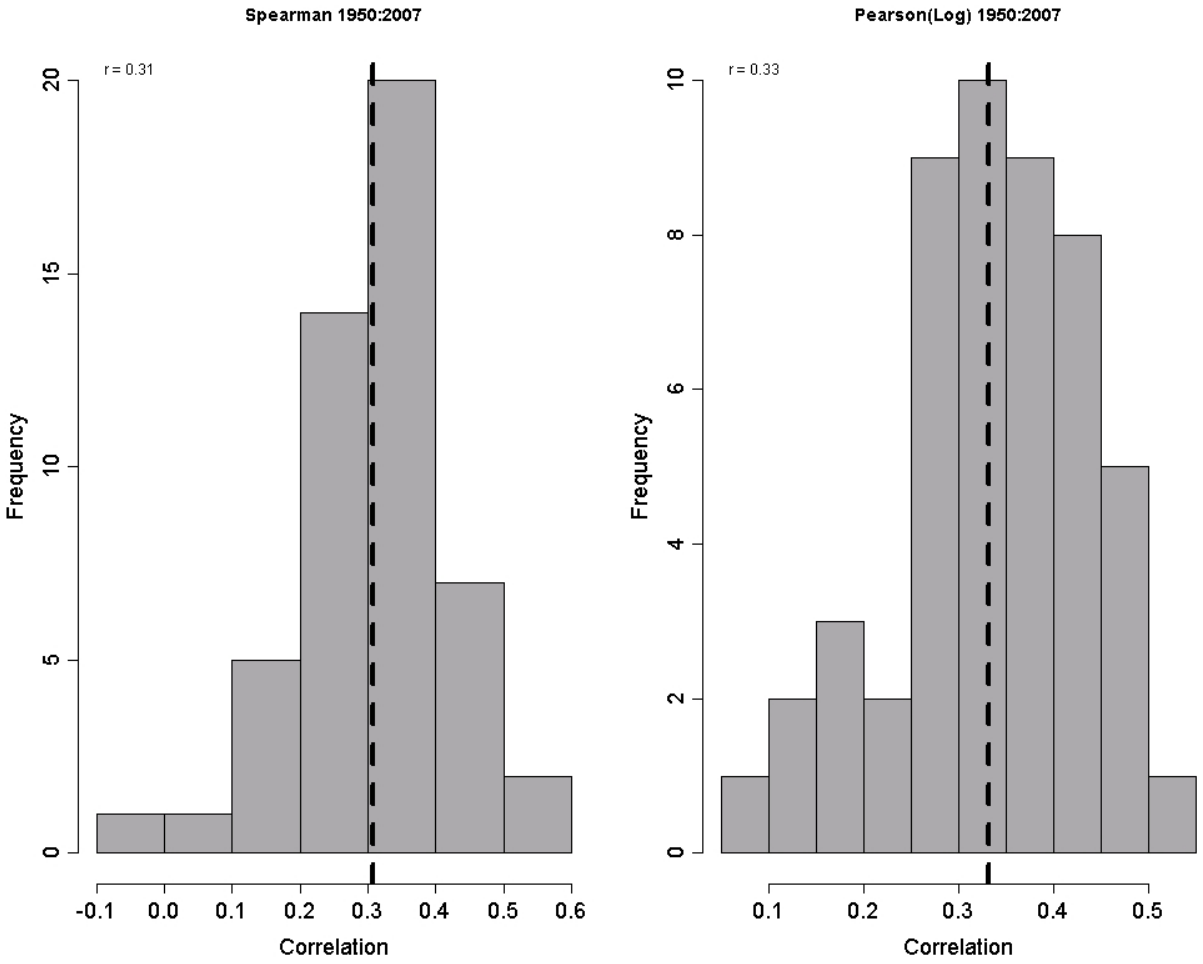

Figure A-5: Maximum area burned for historical data (vertical black line) and simulated (grey histogram) results. The simulation does a good job of representing the maximum annual fire event across the time period of interest for the simulation.

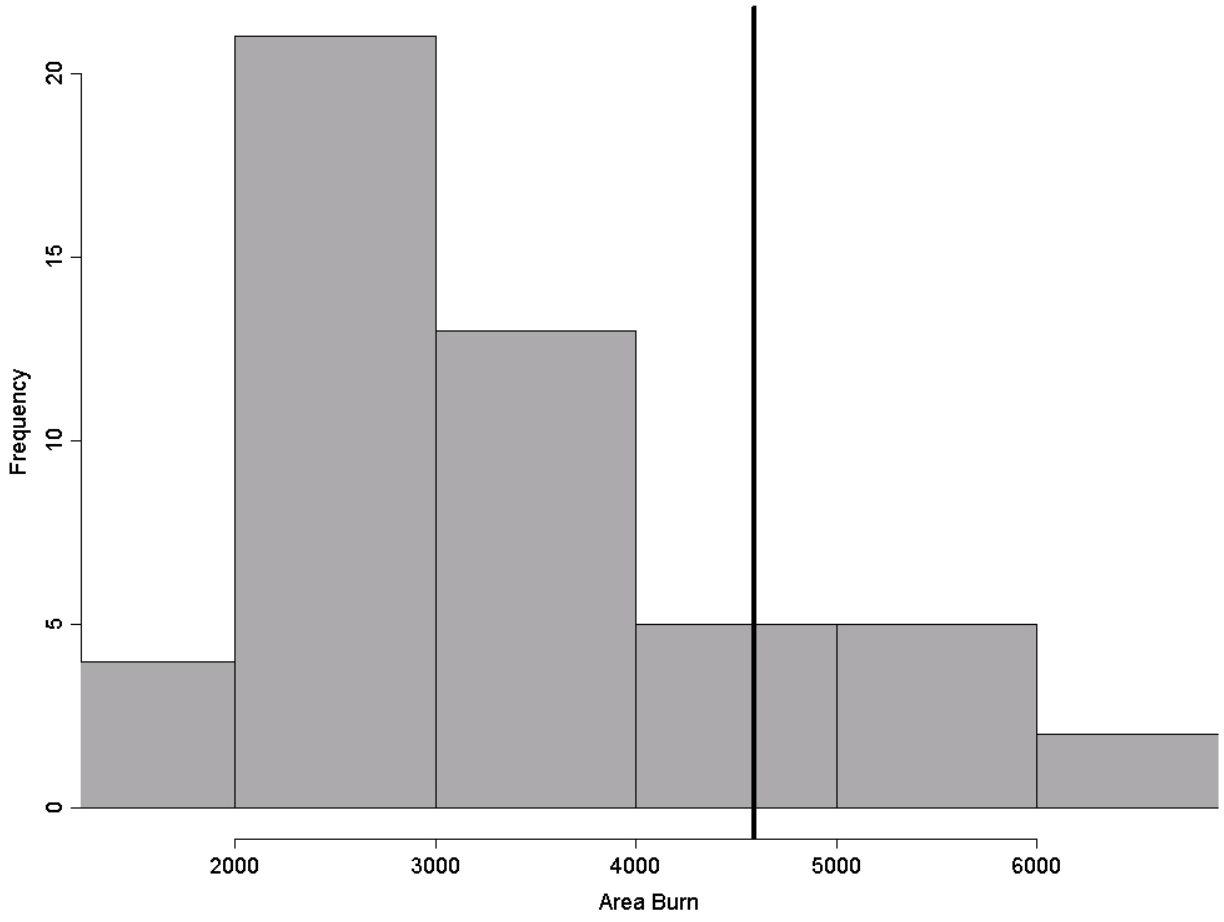

Figure A-6: Maximum fire size event for historical data (vertical black line) and simulated (grey histogram) results. The simulation does a good job of representing the distribution of the largest fires across the time period of interest for the simulation.

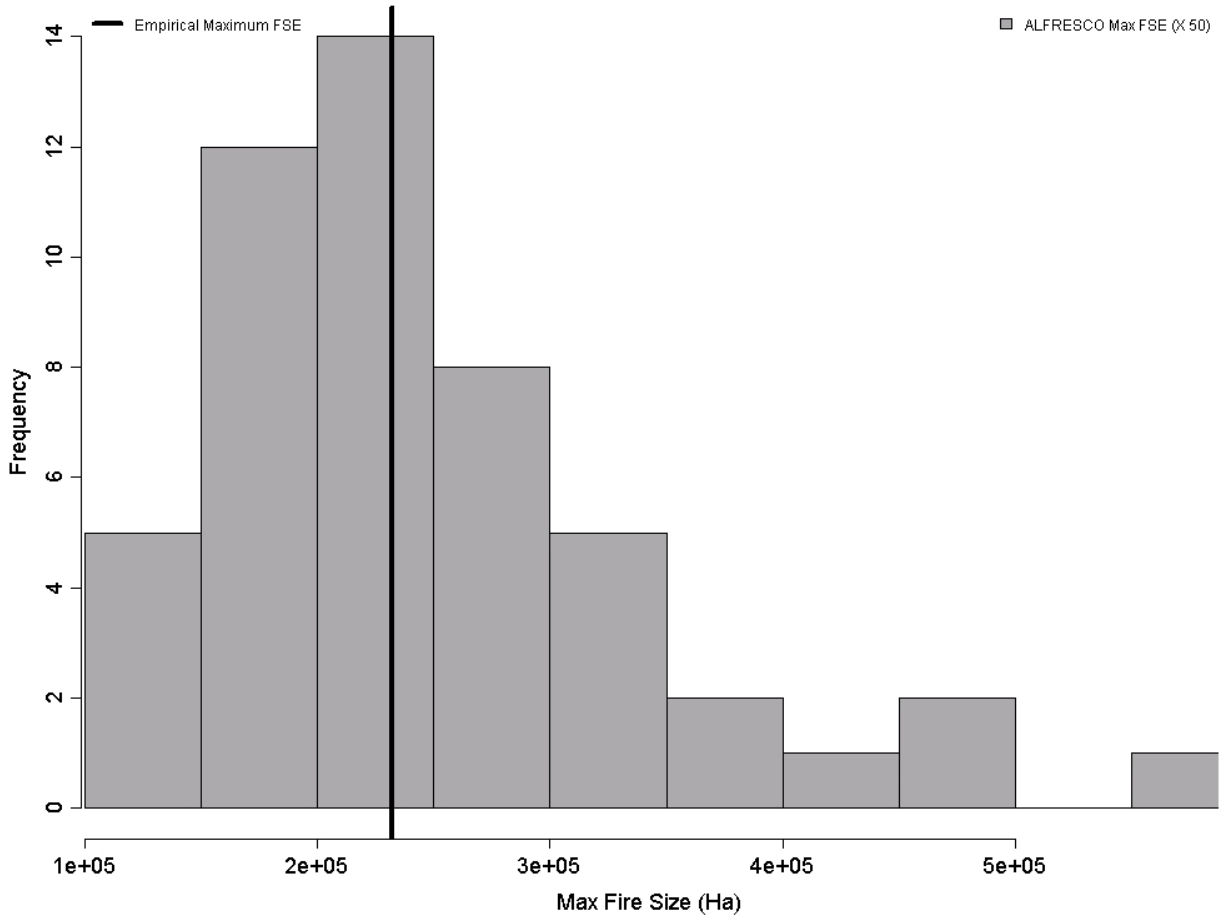

Figure A-7: Mean annual area burned for historical data (vertical black line) and simulated (grey histogram) results. The simulation does a good job of representing the distribution average annual area burned across the time period of interest for the simulation.

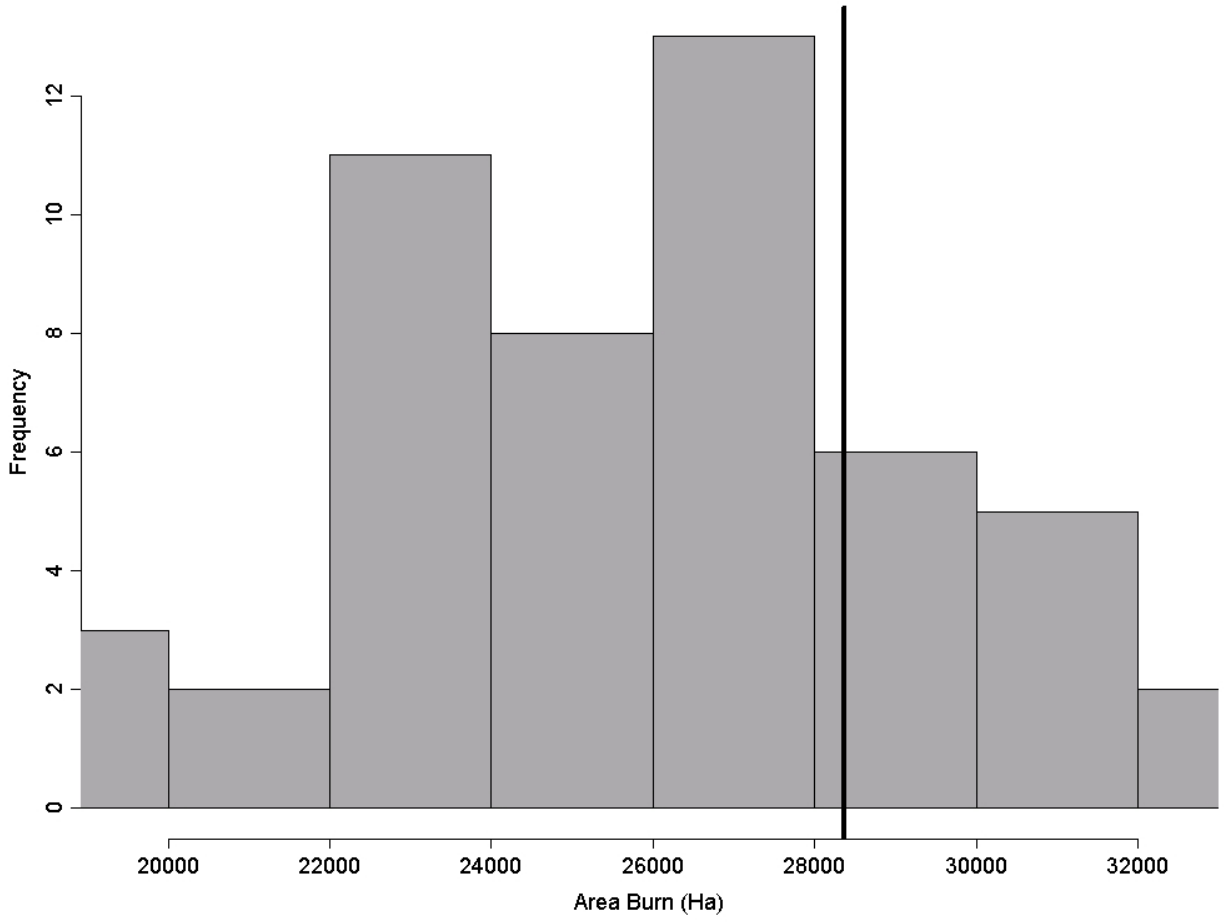

Figure A-8: Mean annual area burned in the spruce trajectories for historical data (vertical black line) and simulated (grey histogram) results. The simulation does a decent job of representing the distribution average annual area burned for the spruce trajectories across the time period of interest for the simulation. There is a slight bias for overburning in the spruce trajectories.

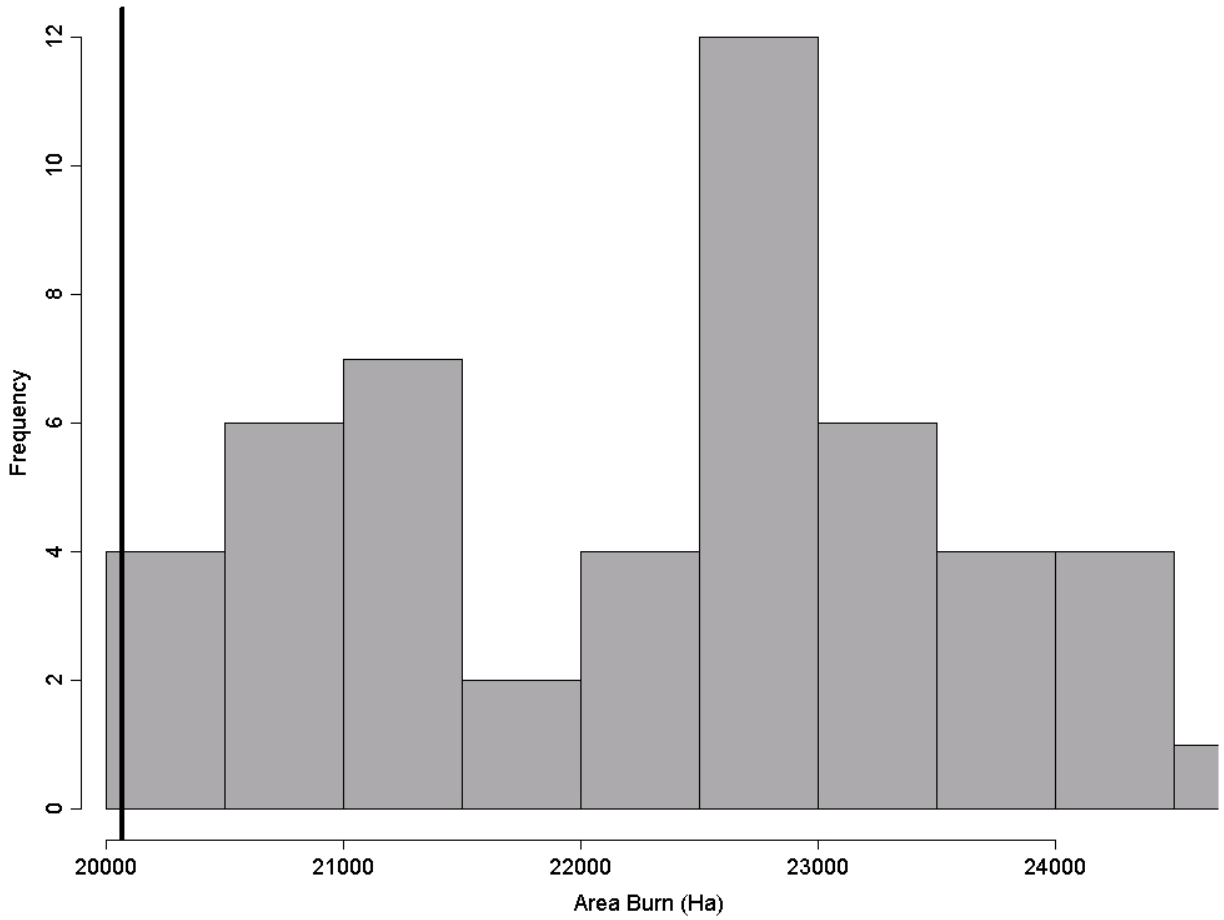

Figure A-9: Mean annual area burned in the tundra trajectories for historical data (vertical black line) and simulated (grey histogram) results. The simulation does a good job of representing the distribution average annual area burned for the tundra trajectories across the time period of interest for the simulation.

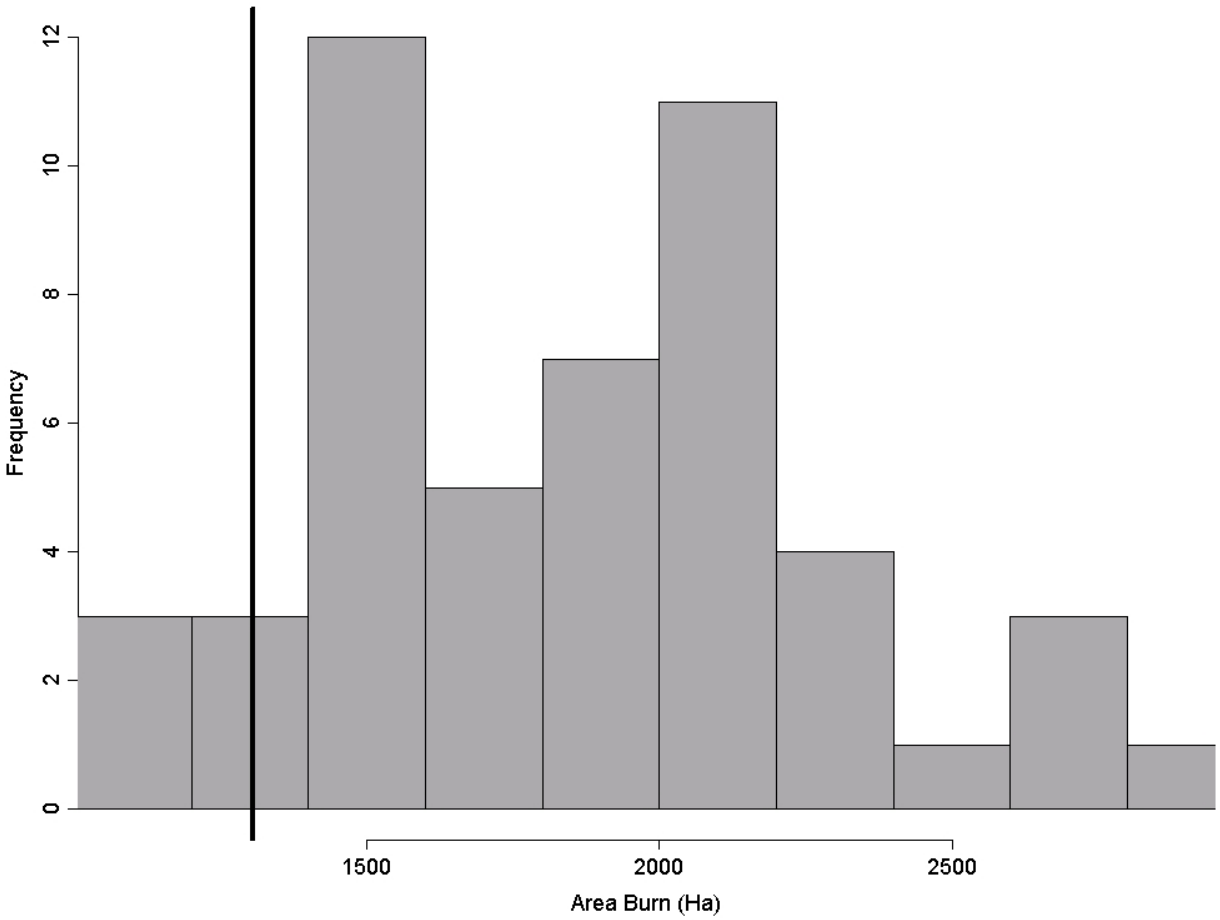

Figure A-10: Ratio of conifer to deciduous cells on the landscape for historical data (vertical black line) and simulated (grey histogram) results. Although the simulation does a reasonable job of representing the ratio of conifer to deciduous cells on the landscape across the time period of interest for the simulation, there is some bias in the model output. These results warrant further investigation as to the source of this discrepancy.

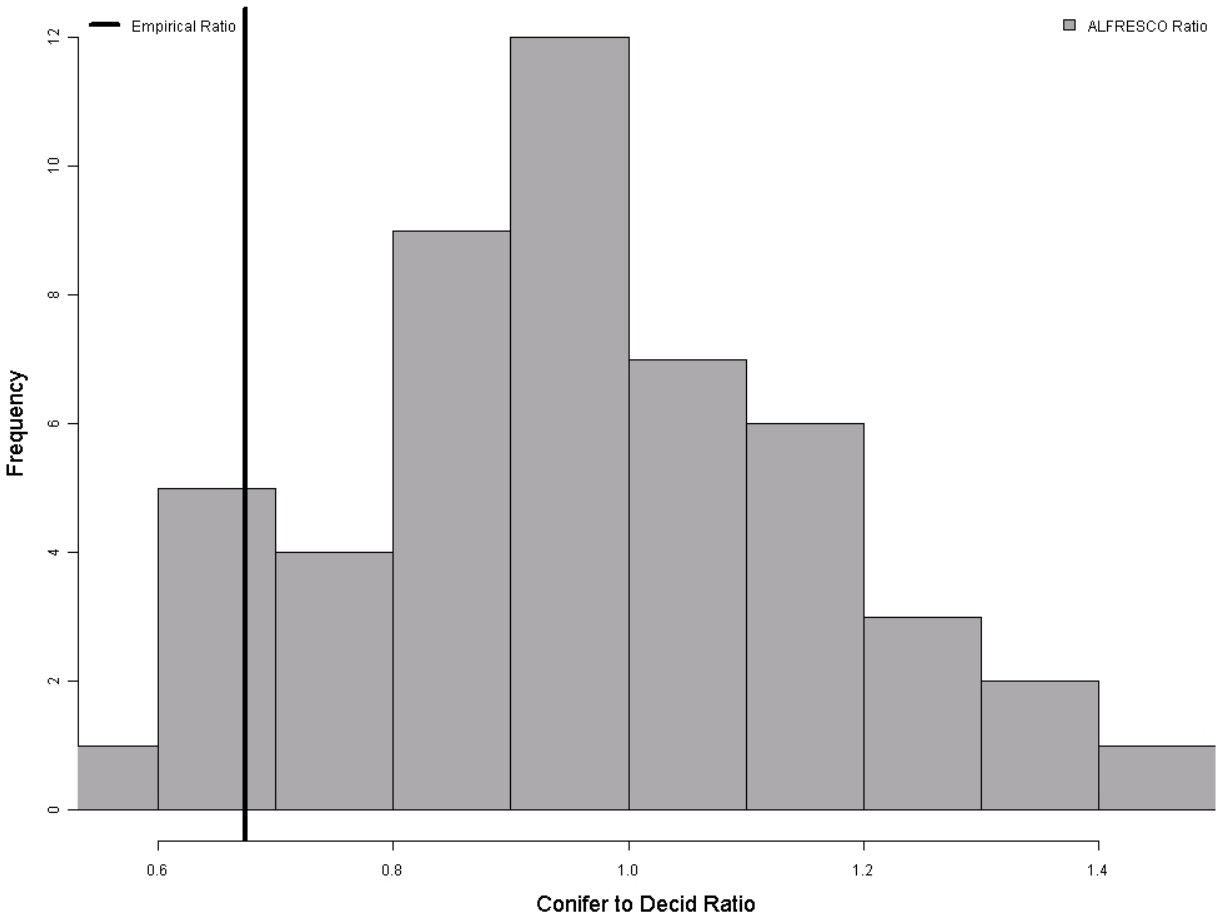

Figure A-11: Example output of a time since fire map for a single replicate on the simulated Kanuti domain. Colors represent time since fire in the legend. The area in black did not burn during the course of the simulation. This plot gives a sense for the type of vegetation patch sizes that are created by the interaction among the recursive burn algorithm and the stochastic succession routine.